**Comparison of ICRF and NBI heated plasmas performances in the JET ITER-like wall**

M.-L. Mayoral, T. Pütterich, P. Jacquet, E. Lerche, D. Van-Eester, V. Bobkov, C. Bourdelle, L. Colas, A. Czarnecka, J. Mlynar, R. Neu, and JET-EFDA Contributors


# Comparison of ICRF and NBI heated plasmas performances in the JET ITER-like wall

M.-L. Mayoral, T. Pütterich, P. Jacquet, E. Lerche, D. Van-Eester, V. Bobkov, C. Bourdelle, L. Colas, A. Czarnecka, J. Mlynar, R. Neu, and JET-EFDA Contributors

Citation: AIP Conference Proceedings **1580**, 231 (2014); doi: 10.1063/1.4864530
View online: http://dx.doi.org/10.1063/1.4864530
View Table of Contents: http://scitation.aip.org/content/aip/proceeding/aipcp/1580?ver=pdfcov
Published by the AIP Publishing

# Comparison of ICRF and NBI Heated Plasmas Performances in the JET ITER-Like Wall

M.-L. Mayoral[a,b], T. Pütterich[c], P. Jacquet[b], E. Lerche[e], D. Van-Eester[e], V. Bobkov[c], C. Bourdelle[e], L. Colas[e], A. Czarnecka[f], J. Mlynar[g], R. Neu[a,c] and JET-EFDA Contributors*

*JET-EFDA, Culham Science Centre, OX14 3DB, Abingdon, UK.*
*[a]EFDA Close Support Unit, Garching, Germany.*
*[b]Euratom/CCFE Association, Culham Science Centre, Abingdon, OX14 3DB, UK.*
*[c]Max-Planck-Institut für Plasmaphysik, EURATOM-Assoziation, Garching, Germany.*
*[d]Association EURATOM-Belgian State, ERM-KMS, Brussels, Belgium.*
*[e]CEA, IRFM, F-13108 Saint-Paul-Lez-Durance, France*
*[f]Association Euratom-IPPLM, Hery 23, 01-497 Warsaw, Poland.*
*[g]Association Euratom-IPP.CR, Institute of Plasma Physics AS CR, 18200 Prague, Czech Rep.*

**Abstract.** During the initial operation of the JET ITER-like wall, particular attention was given to the characterization of the Ion Cyclotron Resonance Frequency (ICRF) heating in this new metallic environment. In this contribution we compare L-modes plasmas heated by ICRF or by Neutral Beam Injection (NBI). ICRF heating as expected led to a much higher centrally peaked power deposition on the electrons and due to the central fast ion population to stronger sawtooth activity. Surprisingly, although a higher bulk radiation was observed during the ICRF phase, the thermal plasma energy was found similar for both cases, showing that a higher radiation inside the separatrix was not incompatible with an efficient central heating scheme. The higher radiation was attributed to the presence Tungsten (W). Tomographic inversion of SXR emissions allowed a precise observation of the sawtooth effect on the radiation pattern. W concentration profiles deconvolved from SXR emission showed the flattening of the profiles due to sawtooth for both heating and the peaking of the profiles in the NBI case only hinting for extra transport effect in the ICRF case.

**Keywords:** JET, ITER-like wall, ICRF heating, impurities, sawtooth
**PACS:** 52.25.Xz, 52.35.Hr, 52.40.Hf, 52.40.Kh, 52.50.Qt, 52.55.Fa

## INTRODUCTION

Following the change of the JET wall from carbon to a tungsten (W) and beryllium (Be) wall [1], detailed studies of the heating systems behavior and performance in such a new metallic environment, were performed [2][3]. In this contribution, we focus on comparing the overall plasma response to 3.5 MW of Ion Cyclotron Resonance Frequency (ICRF) heating with the same amount of heating power from the Neutral Beam Injection (NBI) systems in the newly installed JET ITER-like Wall (JET-ILW). A complementary statistical analysis over a large set of pulses can be found in [4]. The pulse studied here was in L-mode with a magnetic field of 2.55T and a plasma current of 2.46 MA. The operating central electron density was set deliberately to a low value ($2.4\ 10^{19}$ $m^{-3}$) in order to maximize the impurities level which increases with lower edge density [5] and emphasize effects observed. The ICRF heating scheme was hydrogen (H) minority in deuterium (D) with an H concentration of 5.5%. Details on the effect of the H level on the plasma behavior can be found in [6]. Waves were launched with a symmetric spectra ("dipole" phasing; main parallel wave number $k_{//} \approx 6.6$ $m^{-1}$). An ICRF frequency of 42.5MHz was used, leading to an H cyclotron resonance on-axis at 2.8 m (the plasma center was at 2.93 m).

## PULSE OVERVIEW

An overview of the pulse studied (JET pulse 81852) is shown on FIG. 1. The ICRF led to much higher central electron temperature $T_{e0}$ (see also FIG. 2) with maximum values up to 5.7 keV for the ICRF phase and 2.8 keV for the NBI one. This is in agreement with the power deposition of the H minority ICRF heating leading to a centrally

* See the Appendix of F. Romanelli et al., Proceedings of the 24th IAEA Fusion Energy Conference, 2012, San Diego, USA

*Radiofrequency Power in Plasmas*
AIP Conf. Proc. 1580, 231-234 (2014); doi: 10.1063/1.4864530

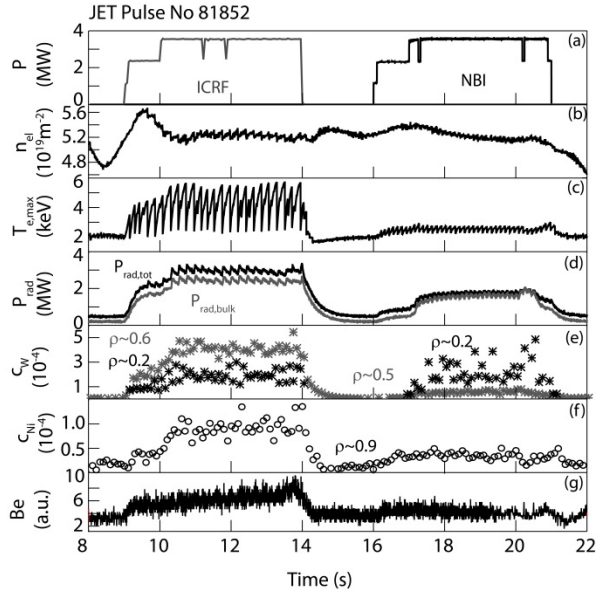


**FIGURE 1** (a) ICRF and NBI power, (b) central line integrated density (c) central electron temperature $T_{e0}$, (d) total and bulk radiated power, (e) W concentration (from spectroscopic measurements [8]), (f) NI concentration (from spectrometric measurements [5] and (g) photon flux Be II 527nm (outer divertor).

peaked electron power deposition and of the NBI heating leading, with the voltage (80kV) and injection (2 beams with tangency radius of 1.31m off-axis, 1 beam with tangency radius of 1.85m on-axis) used, to a broad power deposition mainly to the ions (see FIG. 4) The sawtooth activity was much stronger in the ICRF phase (period ~ 200ms, $T_{e0}$ drops by up to 57%) than in NBI phase (130ms, $T_{e0}$ drops by up to 20%). This is consistent with sawtooth stabilization by the ICRF-accelerated H population when the minority resonance layer is situated centrally [7]. A higher total radiated power (see FIG.1) was also obtained for the ICRF with, as for the NBI, most of the radiation coming from inside the last closed flux surface (estimated from bolometers and referred here as the bulk radiation $P_{rad,bulk}$). W was identified as the main radiator. The W concentration $c_W$, was calculated from spectrometers at to 5 nm where a strong spectral feature of the W-ions $W^{27+}$ to $W^{35+}$ is emitted [8]. The special feature, referred as "quasi-continuum" is emitted at $T_e \approx 0.8$-1.8 keV, i.e. towards the plasma edge (see grey point on FIG. 1e). Additionally, a more central $c_W$ can be obtained from the line radiation of $W^{42+}$ to $W^{45+}$ near 6 nm. As represented on FIG. 1e, $c_W$ was found similar on the plasma center ($2\ 10^{-4}$ at $\rho \approx 0.2$) for both the NBI and ICRF heating phases and higher towards the edge ($\rho \approx 0.5$ - 0.6) for the ICRF. These data gave us a first hint of a very different W behavior for both heating methods: the ICRF having a higher overall level but without peaking as for the NBI. The nickel (Ni) concentration at the edge ($\rho \approx 0.9$) was estimated from spectroscopic measurements (see [5]) and was found to be higher in the ICRF phase (see FIG. 1f). This is consistent with JET C-wall results for which ICRF heating was also leading to higher Ni level. In this pulse, one could estimate that the Ni contributed to only 1% of the radiated power. Note that the dependence of the radiated power to $T_e$ via $R_W$, the cooling factor of the W, i.e. $P_{rad,bulk} = n_e^2\, c_W\, R_W(T_e)$ can be a factor influencing the higher radiation in the ICRF case. Nevertheless, as shown in [8], the W cooling factor dependence on $T_e$ is rather weak at this temperature level and in any case, the attempt to match $T_e$ in both heating phase was always hampered by the sawtooth activity in the ICRF phase.

## PLASMA PERFORMANCE

Additionally to the significant increase in $T_e$, that came as a proof of an efficient heating scheme, the plasma energy from magnetic measurement $W_p$, was also found significantly higher in the ICRF case even though the radiated power was also higher. This is shown on FIG 3. Note that ion temperature was not available for this pulse and that the thermal energy represented on FIG. 3b was evaluated by removing the fast ion contribution, $W_{fast}$, from $W_p$ using the following formula $W_{th} = W_p - 0.75W_{fast,\perp} - 1.5W_{fast,//}$ with $W_{fast,\perp}$ an d $W_{fast,//}$ the perpendicular and parallel fast ions contributions, / were evaluated the from TORIC [9] and NUBEAM [10])codes both installed in TRANSP [11]. As expected, for the ICRF the fast ion energy was higher and when their contribution was removed, the thermal energy in the two heating phases was found similar. The difference between the total thermal loss power defined as $P_{loss} = P_{Ohmic} + P_{ICRF} + (P_{NBI} - P_{CX} - P_{shine\text{-}through}) - dW_{dia}/dt$ and $P_{rad,bulk}$ was smaller in the ICRF case (≈ 2.4 MW) than in the NBI case (≈ 3 MW). Assuming a standard scaling law dependence $W_{th} = C \times (P_{loss} - P_{rad,bulk})^{0.3}$ with C a constant evaluated from the NBI phase the difference ($P_{loss}$-$P_{rad,bulk}$) in the ICRF phase should give a thermal energy in the range of 0.7 MJ. The value

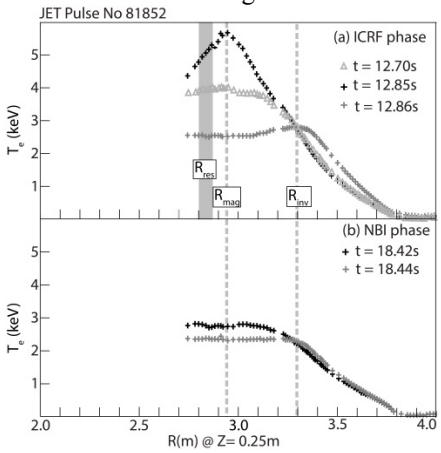


**FIGURE 2** Typical evolution of $T_e$ profiles during a sawtooth crash.

obtained experimentally of 0.75 MW show that higher radiating losses do not necessarily mean degraded confinement. Interestingly when plotting the difference between the total power deposited by the ICRF /NBI and the bulk radiated power, both volume integrated, one can clearly see the higher radiation during ICRF is "compensated" by the more central power deposition (see FIG. 4).

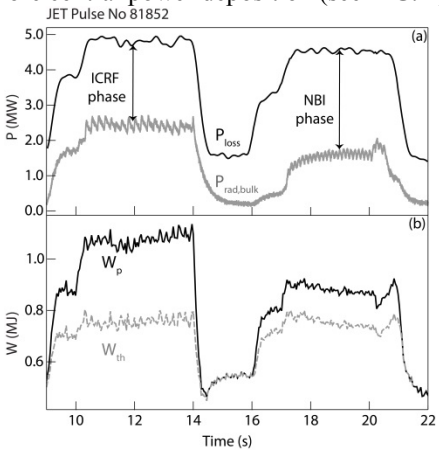


**FIGURE 3:** (a) Total thermal loss power and bulk radiation (b) plasma energy $W_p$ and thermal energy $W_{th}$.

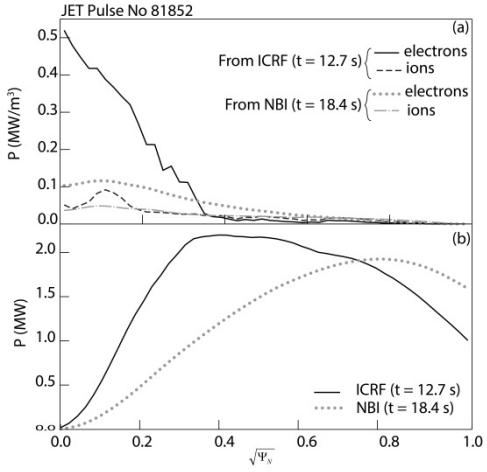


**FIGURE 4:** (a) Electrons and ions power deposition profiles. (b) Difference between volume integrated total deposited power and $P_{rad,bulk}$ (assuming a flat profile). The x-axis is square root of the normalized toroidal flux

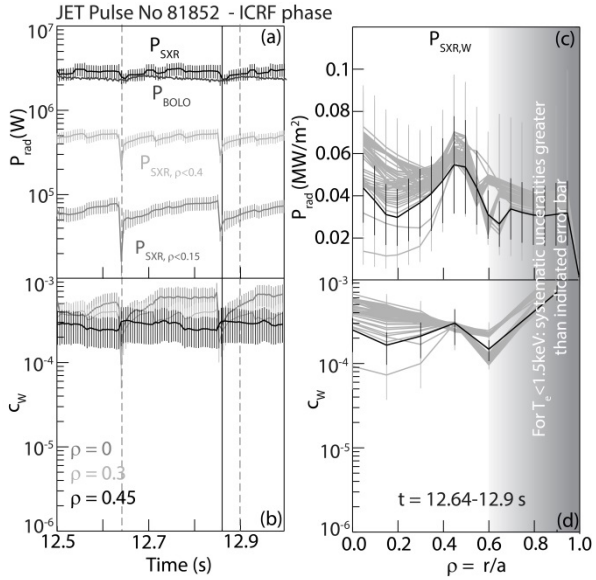


**FIGURE 5.** Time evolution of (a) $P_{rad,bulk}$ (vertical bolometers) and $P_{rad}$ inside ρ = 0.15, 0.4, 1 (from SXR); (b) $c_W$ at ρ= 0.15, 0.3, 0.45. Profiles evolution for t = [12.64 -12.9] s every 5 ms of (c) $P_{rad}$ from W (from SXR) and (d) $c_w$. The black profiles on (c) and (d) correspond to the black line on (a) & (c)

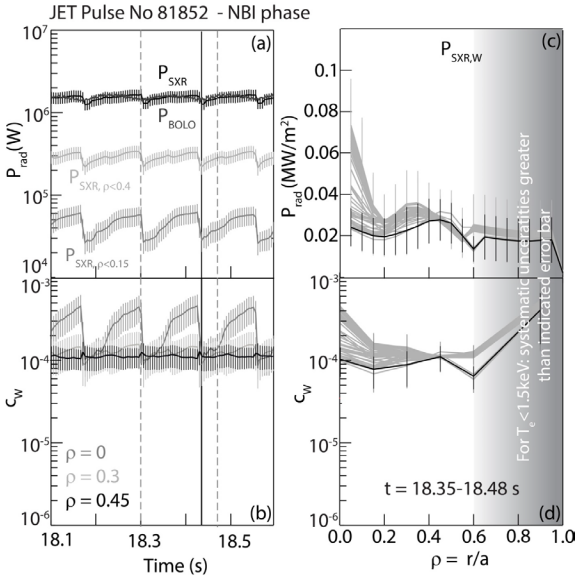


**FIGURE 6** Time evolution of (a) $P_{rad,bulk}$ (vertical bolometers) and $P_{rad}$ inside ρ = 0.15, 0.4, 1 (from SXR); (b) $c_W$ at ρ = 0.15, 0.3, 0.45. Profiles evolution for t = [18.1 -18.6] s every 5 ms of (c) $P_{rad}$ from W (from SXR) and (d) $c_w$. The black profiles on (c) and (d) correspond to the black line on (a) & (c)

## W IMPURITY BEHAVIOUR

In order to look in a more detailed way at the evolution of the W profiles taking into account the changes triggered by the sawtooth activity, a deconvolution of the SXR emission was performed. The method, described in [12], involved removing the bremsstrahlung emission (estimated from experimental measurements of $T_e$, $n_e$, $Z_{eff}$) from the SXR emission (the rest assumed to be from W). From the results shown on FIG. 5 (ICRF) and FIG. 6 (NBI) several

conclusions could be drawn. Firstly, the total radiated power inside a normalised radius ρ of 0.15, $P_{rad,\rho<0.15}$, could be as high in the NBI as in the ICRF case (see FIG. 5a and 6a) even if further out it was lower. Secondly, the effect of the sawtooth crashes could be seen for both heating cases with the W profiles flattening within the sawtooth inversion radius (≈ 0.4) after the crashes (see for example, the black line on FIG. 5 & 6, plots c and d). Note that validity of hollow profiles that follows the first sawtooth crash in the ICRF case is still under scrutiny. Finally, as seen from the spectrometer data, the NBI led to peaked W concentration, within ρ of 0.15. This could be seen on the profiles on FIG. 6d and FIG. 6c but also on FIG. 6b where in the middle of each sawtooth $c_W$ at ρ = 0 became significantly higher than $c_W$ at ρ = 0.3 and ρ = 0.45.

## SUMMARY

Intrinsic differences between the ICRF and NBI heating like the power deposition profiles, led a much higher electron temperature in the ICRF case and stronger sawtooth effect. The higher W content in the ICRF (see [3-5]) led to higher bulk radiation. Nevertheless similar thermal plasma energies were obtained in both cases. This is consistent with the fact that in the ICRF case the power is centrally deposited and the radiated power reveals flatter profiles. In the investigated pulse, the sawtooth activity clearly affects positively the impurities with a stronger effect during ICRF. During the NBI phase, although the overall W level oscillates at a lower value than in the ICRF case, W peaking within ρ of 0.15 is observed. This was also observed in H-mode [3]. The fact that peaking is not observed during the ICRF, hints to a beneficial effect of higher temperature gradient on impurities transport as observed on AUG [13][14], JET C-wall with Ar & Ni [15][16] and more recently with H-modes in JET with the ILW [3] although for the later only preliminary results are obtained and more data should come for the next JET-ILW experimental campaign.

## ACKNOWLEDGMENTS

This work, supported by the European Communities under the contract of Association between EURATOM and CCFE, was carried out within the framework of the European Fusion Development Agreement. The views and opinions expressed herein do not necessarily reflect those of the European Commission. This work was also part-funded by the RCUK Energy Programme under grant

## REFERENCES

[1] Philipps V *et al.,* 2010 "Overview of the JET ITER-like Wall Project" Fus. Eng. and Design **85** 581–1586.
[2] Mayoral M-L *et al.,* 2012 "On the Challenge of Plasma Heating with the JET Metallic Wall" Proc. of 24th IAEA Fusion Energy Conference, San Diego, USA- EX/4-3.
[3] Jacquet P *et al.,* 2013 "ICRF heating in JET during initial operations with the ITER-like wall", this conference.
[4] Lerche E *et al.*, 2013 "Statistical analysis of the ICRF and NBI heating performances in L-mode at JET", this conference.
[5] Czarnecka A *et al.* 2013 "Spectroscopic Investigation of Heavy Impurity Behaviour During ICRH with the JET ITER-Like Wall", this conference.
[6] Van Eester D *et al*., 2013 "Hydrogen minority ion cyclotron resonance heating in presence of the ITER-like wall in JET", this conference.
[7] Chapman I *et al.*, 2007 "The physics of sawtooth stabilization" Plasma Phys. Control. Fusion **49** B385–B394.
[8] Pütterich T *et al.,* 2010 "Calculation and experimental test of the cooling factor of tungsten" Nucl. Fusion **50** 025012
[9] Brambilla M., 1999 "Numerical simulation of ion cyclotron waves in tokamak" Plasmas Plasma Phys. and Control. Fusion **41** 1–34
[10] Pankin A *et al.,* 2004 "The tokamak Monte Carlo fast ion module NUBEAM in the National Transport Code Collaboration library" Comput. Phys. Commun. **159** 157
[11] Goldston R J *et al.*, 1981 "New techniques for calculating heat and particle source rates due to neutral beam injection in axisymmetric tokamaks" J. Comput. Phys.**43** 61
[12] Pütterich T *et al.,* 2013 "W screening and Impurity control in JET" Proc. of 24th IAEA Fusion Energy Conference, San Diego, USA - P3-15.
[13] Dux R *et al.*, 2003 Influence of the heating profile on impurity transport in ASDEX Upgrade" Plasma Phys. and Control. Fusion **45** 1815–1825.
[14] Sertoli *et al*., 2011 "Local effects of ECRH on argon transport in L-mode" Plasma Phys. and Control. Fusion **53** 035024 (21pp).
[15] Puiatti M. *et al.*, 2003 "Simulation of the time behaviour of impurities in JET Ar-seeded discharges and its relation with sawtoothing and RF heating", Plasma Phys. and Control. Fusion **45** 2011–2024.
[16] Puiatti M. et al 2006, "Analysis of metallic impurity density profiles in low collisionality JET H-mode and L-mode plasmas", Physics of Plasmas **13** 042501.